IEEE Access
Multidisciplinary ⋮ Rapid Review ⋮ Open Access Journal

Received 10 May 2024, accepted 22 May 2024, date of publication 19 June 2024, date of current version 3 November 2025.

Digital Object Identifier 10.1109/ACCESS.2024.3416464

METHODS

Performance Evaluation of Cooperative Spectrum Sensing Algorithm Based on Quantum Manta Ray Algorithm

JUN CHEN[1], YIPING HUANG[1], TIANYI WANG[2], LING ZHANG[1], AND YUQIAN LI[2]
[1]Chengdu Fuyuanchen Technology Company Ltd., Chengdu 610037, China
[2]China Research Institute of Radiowave Propagation, Qingdao 266107, China

Corresponding author: Yuqian Li (liyuqian1025@foxmail.com)

ABSTRACT In order to address the issue of limited sensing accuracy in traditional spectrum sensing algorithms within low SNR communication environments, a novel multi-node cooperative sensing method is proposed in this work. In this approach, each node utilizes a stochastic resonance sensing model for information detection, while the OR criterion is employed to fuse information from multiple nodes. In situations where user presence cannot be reliably determined, each node simultaneously transmits signal energy values and SNR for weighted fusion. Morevover, the weighted fusion stage focuses primarily on determining the weight coefficients of each node. To achieve this efficiently, a Quantum Manta-Ray Optimization Algorithm capable of selecting these weights effectively, is proposed. While comparing with the other existed methods, this method can exhibits superior sensing efficiency and get the excellent sensing performance. The algorithm's perceptual accuracy is enhanced by over 5%.

INDEX TERMS Spectrum sensing, stochastic resonance, cognitive radio, energy detection algorithm.

I. INTRODUCTION

The exponential growth in the user base of radio networks has created significant challenges and put immense pressure on wireless communication networks in the era of information technology [1]. However, the radio spectrum, encompassing electromagnetic wave frequencies ranging from 0 to 3000GHz, is a limited non-renewable resource in the natural environment. As society advances, there is an increasing demand for radio spectrum, leading to its depletion and exacerbating conflicts between demand and availability. This highlighting the pressing need to address this issue in a smoother and rigorous manner that aligns with the requirements set by Nature Journal [2]. With the Internet era's advent, people's proficiency and reliance on wireless communication equipment are escalating [3]. However, at this stage, the insufficient allocation of spectrum resources fails to meet users growing demands, consequently leading to increasingly instensified conflicts. Consequently, the inability of the idle spectrum to meet the demand become an urgent problem that countries urgently must overcome [4], [5], [6].

Moreover, Cognitive Radio was proposed by Mitola which is a new theory, and applied low spectrum utilization [7], [8]. It is mainly a kind of radios that can dynamically observe and learn from the surrounding electromagnetic environment, and autonomously allocate and control spectrum resources dynamically according to the current spectrum resource obtained from the perception [9]. The primary objective of the CR technology is to efficiently allocate the available authorized frequency band to secondary users upon detecting underutilization by primary users, leading to facilitate optimal utilization and sharing of spectrum resources. Moreover, this technology can significantly enhance spectrum utilization rates. However, at the level of spectrum sharing allocation, it becomes imperative to consider potential interference caused by sub-users on primary users. Hence, sub-users must adhere to interference constraints while occupying authorized frequency bands to ensure uninterrupted communication and information transmission for primary

The associate editor coordinating the review of this manuscript and approving it for publication was Yun Lin.

users [10]. Furthermore Cognitive Radio is widely used not only in the signal recognition but also other fields [11], [12]. Spectrum sensing serves as the initial stage of cognitive radio, with the primarily objective of understanding the wireless environment to identify spectrum gaps and then transmitting this information to cognitive users [13], [14]. Two main types of perception algorithms exist, single-user perception algorithms and multi-user cooperative perception algorithms. The former includes three classic types of perception algorithms are energy detection algorithms [15], matched filter perception algorithms [16], [17], [18] and cyclic smooth detection algorithms [19]. The energy detection algorithm is computationally efficient and straightforward not requiring the prior knowledge of the detection signal for perception. However, its performance degrades significantly in low SNRs scenarios [20].

Literature [21] proposes an enhanced energy detection algorithm tailored for intelligent reflecting surfaces incorporating spectral sensing and considering the direct link between primary users and the secondary users. Additionally, a cooperative spectrum sensing method and the method of multiple Intelligent Reflecting Surfaces(IRS) are suggested to enhance the sensing method. Experimental results affirm the superior performance of the proposed sensing algorithm. Literature [22] introduced a novel approach by proposing the utilization of median absolute deviation statistic for estimating the noise variance in threshold evaluation. Through a comparative analysis of experimental results, it becomes evident that the method has been proposed in this paper outperforms both traditional energy detection algorithms and deep learning-based detection algorithms. Moreover, the cyclic smooth feature detection algorithm analyzes the correlation function of the signal spectrum. In literature [23],a spectrum sensing algorithm utilizing cyclic smooth feature detection and Hilbert transform is presented. The proposed algorithm demonstrates effective signal-type detection even in low SNRs scenarios, exhibiting superior sensing performance. Nevertheless, the cyclic smooth detection algorithm's higher complexity and longer detection time make it challenging to the of agile spectrum sensing in CR.

Aiming to address the issue of poor perception performance among single node users, several scholars have proposed collaborative spectrum perception methods. These methods consist primarily of two types of algorithms: centralized collaborative sensing and distributed collaborative sensing [24], [25], [26]. The two perception algorithms constitute a collaborative perception architecture in which each node senses the channel and then fuses the sensed information. Compared to the traditional single-node perception algorithm, the multi-node collaborative perception algorithm can significantly improve the effectiveness of spectrum perception. However, there are several areas within the collaborative approach and information fusion that require further improvement.

Energy detection algorithm plays an important role in cognitive radio. literature [27] presented a low-complexity and energy-efficient method for sensor selection during cooperative spectrum sensing. This approach aimed to minimize the energy consumption of the cooperative spectrum sensing scheme through the selection of only a minimum number of sensing nodes. Furthermore, the computational complexity introduced in literature A was significantly reduced compared to traditional algorithms. Addressing the challenge of countering spectrum sensing data forgery attacks, literature [28] introduced a distributed cooperative sensing algorithm. This algorithm considers each secondary user as an agent and employs reinforcement learning to facilitate its interaction with neighboring nodes. Experimental results demonstrate that the proposed algorithm effectively detects and mitigates interference caused by malicious users. Recognizing the susceptibility of single node sensing to noise uncertainty, literature [29] proposes a cooperative spectrum sensing algorithm that applies energy detection and Sevcik fractal dimension. The adaptive threshold energy detection algorithm is used for signal detection and judgment. Simulation results demonstrate superior detection performance under noise uncertainty compared to other algorithms. Moreover literature [30] proposes a collaborative energy detection algorithm that enhances perception by applying only the mean and variance of the detection statistics. The authors substantiate the efficacy of the algorithm in various prevalent fading scenarios, including slow fading, block fading, and fast fading. Simulation results showcase that this proposed algorithm significantly outperforms traditional spectrum sensing algorithms.

Despite the extensive research conducted by scholars on spectrum sensing algorithms and the proposal of more effective alternatives to traditional methods, challenges persist in terms of poor sensing performance and unsatisfactory detection accuracy, particularly in low SNR environments. The perception algorithm, being the fundamental technology in cognitive radio (CR), serves as the basis for achieving spectrum allocation. [31] To address the issue of inadequate performance exhibited by existing spectrum sensing algorithms under low SNR conditions, this paper investigates and enhances traditional energy detection algorithms to mitigate the impact of low SNR and enhance overall sensing performance.

This paper presents a novel multi-node cooperative perception algorithm, the Multiple Stochastic Resonance Algorithm(MSRA). For single-node perception, a model based on stochastic resonance is employed, while for multi-node cooperative perception, a model solved by intelligent algorithms is utilized to enhance perception effectiveness. The performance of MSRA is validated by comparing it to cutting-edge perception algorithm under low SNR. Since MSRA is a multi-node collaborative perception algorithm, it can alleviate some of the perception errors or malicious attacks that users may encounter [32]. To sum

up, the primary contributions of this study are outlined as follows:

- The stochastic resonance algorithm is employed as a single-node sensing model, integrated into the multi-node cooperative sensing framework to enhance accuracy in scenarios with a low SRN scenarios.
- The quantum manta ray algorithm is applied for weight selection in the multi-node cooperative sensing algorithm, aiming to acquire enhanced weights leading to improved sensing outcomes.

II. ENERGY DETECTION SENSING MODEL

In the cognitive radio technology domain, the primary emphasis is focused on proficiently sensing and discerning the presence of authorized spectrum users, known as primary users. When the authorized spectrum is indeed occupied by primary users, secondary users receive signals involving both primary user transmissions and ambient noise. In opposite, when the authorized spectrum is available, secondary users primarily detect noise. Therefore, this spectrum sensing process can be represented as a binary hypothesis model:

$$y(t) = \begin{cases} n(t), & H_0 \\ x(t) \otimes h(t) + n(t), & H_1 \end{cases} \tag{1}$$

where $h(t)$ indicates the channel gain characterized by Gaussian white noise. Moreover, H_0 signifies that the current channel is unoccupied by a primary user, denoting an available authorized spectrum. However, H_1 suggests that the current channel is occupied by a primary user, yielding an unavailable authorized spectrum. In addition, the performance metrics of the binary hypothesis model are primarily characterized by their probability of detection P_d, probability of false alarm P_f, and probability of miss detection P_m.

The detection probability $P_d = P(H_1|H_1)$ quantifies the likelihood of the secondary user accurately in detecting its within the authorized band. Moreover, the false alarm probability represents the likelihood that the secondary user incorrectly determines the authorized band occupation of the primary user, even though the primary user is not using it. In other words, $P_f = P(H_1|H_0)$.

As for the missed detection probability,it refers to the likelihood that the secondary user incorrectly defines that the primary user is not occupying the authorized channel, even though the primary user is utilizing the designated frequency band. This is denoted as $P_m = P(H_0|H_1)$.

Therefore,the single-threshold energy detection algorithm is basically employed to assess the presence of the primary user utilizing Eq. (2) after computing the energy value derived from the sensed signal $y(t)$. This is modelled as follows:

$$D = \begin{cases} H_1, \ T > \lambda \\ H_0, \ T \leq \lambda \end{cases} \tag{2}$$

where λ represents the threshold value of the single threshold energy detection algorithm. Moreover, H_1 denotes the presence of a primary user in the currently detected frequency band, while H_0 reflects the absence of a primary user. Finally, T refers to the detection statistic obtained through Eq. (3):

$$T = \sum_{n=1}^{N} |y(n)|^2, \tag{3}$$

where N represents the total number of sampling points in the sampled signal.

Consider that $n(t)$ represents an additive white Gaussian noise with a zero value and a variance of σ^2. Let T denote the sum of squares of N Gaussian distributions, followings a chi-square distribution. According to the central limit theorem, when N is sufficiently large ($\gg$ 20), the chi-square distribution can be approximated by a Gaussian distribution,denoted as follows:

$$T \sim \begin{cases} N\left(N\sigma^2, 2N\sigma^4\right), \\ N\left(N\sigma^2 + Np_s, 4N\sigma^4 p_s\right), \end{cases} \tag{4}$$

where $p_s = (\sum_{n=1}^{N} |x(n)|^2)/N$ is the average power of the primary user signal. When the sensing threshold λ of the energy detection algorithm is fixed and a sufficiently large sampling point is selected, one can identify the false alarm probability and the detection probability of the secondary user, defined as follows:

$$P_d = P(T > \lambda|H_1) = Q\left(\frac{\lambda - N(\sigma^2 + p_s)}{\sigma\sqrt{2N\sigma^2 + 4Np_s}}\right), \tag{5}$$

$$P_f = P(T > \lambda|H_0) = Q\left(\frac{\lambda - N\sigma^2}{\sigma^2\sqrt{2N}}\right), \tag{6}$$

where $Q(x) = 1/\sqrt{2\pi}\int_x^{+\infty} e^{\frac{-t^2}{2}} dt$. If the probability of the false alarm is known, the detection threshold can be determined as follows:

$$\lambda = \left[\sqrt{2N}Q^{-1}(P_f) + N\right]\sigma_\omega^2, \tag{7}$$

In the a communication system, most of the noise comprises a collection of independent noises, and what the receiver receives is essentially a mixture of noise and dynamic interference. Changes in location, weather conditions, and time can lead to variations in the noise variance, often referred to as noise uncertainty of noise. Noise uncertainty,denoted as ρ, is mainly used to describe the uncertainty of the current noise variance. Moreover,ρ dynamically changes according to the current channel environment, when the channel conditions are favorable, ρ tends to be relatively small,whereas the channel environment is relatively poor, ρ will be relatively large. After introducing uncertainty E, the actual variance of noise can be expressed as follows:

$$\hat{\sigma}_n^2 \sim \mathrm{U}\left(\frac{\sigma_n^2}{\rho}, \rho\sigma_n^2\right), \tag{8}$$

where $\hat{\sigma}_n^2$ represents the actual variance of the noise, and σ_n^2 denotes the normalized variance of the noise.

After considering the noise uncertainty ρ, the detection probability P_d and the false alarm probability P_f can be obtained:

$$P_d = P(Y > \lambda \mid H_1)_{\min} = Q\left(\frac{\lambda - \left(P + \sigma_n^2/\rho\right)}{\sqrt{2/N}\left(P + \sigma_n^2/\rho\right)}\right), \quad (9)$$

$$P_f = P(Y > \lambda \mid H_0)_{\max} = Q\left(\frac{\lambda - \rho\sigma_n^2}{\sqrt{2/N}\rho\sigma_n^2}\right), \quad (10)$$

where $P = (\sum_{n=1}^{N} |s(n)|^2)/N$ and $s(n)$ is the primary user signal. The double threshold energy detection algorithm primarily determines the existence of the primary user by deploying two distinct thresholds. The precise procedure for making this determination is elucidated as follows:

$$Y = \begin{cases} H_0 & E \le \lambda_{low} \\ Notdecide & \lambda_{low} < E \le \lambda_{high} \\ H_1 & E > \lambda_{high} \end{cases} \quad (11)$$

where λ_{high} indicates the high threshold of the double threshold energy detection algorithm, and λ_{low} denotes the low threshold. When the energy statistic T exceeds λ_{high}, the secondary user perceives that the primary user occupies the currently licensed frequency band. Conversely, when T falls below λ_{low}, it indicates that the secondary user believes that the primary user does not use the authorized frequency band. In cases where $\lambda_{low} < E \le \lambda_{high}$, further assessment is required to determine if the primary user occupies the authorized frequency band.

III. MULTI-MODE COLLABORATIVE SENSING ALGORITHM BASED ON STOCHASTIC RESONANCE

In this section, the double threshold energy detection algorithm is enhanced by incorporating stochastic resonance to address the suboptimal perception results observed in single node perception. Hence, the proposed binary detection model is determined as follows:

$$z(t) = \begin{cases} n(t) + b(t), & H_0 \\ s(t) + n(t) + b(t), & H_1 \end{cases} \quad (12)$$

Reference [33] proposes an optimal stochastic resonance probability density distribution function, expressed as follows:

$$b_\eta^{opt} = \delta(\eta - \beta), \quad (13)$$

where, in a signal with low SNR and small mean, the optimal value β^{opt} is determined as follows:

$$\beta^{opt} = \frac{\mu\sigma_s^2 - \mu\sigma_n^2 - \mu^3}{\mu^2 - \sigma_s^2}, \quad (14)$$

When dealing with single node perception and high dynamic noise, inaccurate perception results and poor perception effects may persevere. Therefore, to enhance spectrum sensing performance in a high dynamic noisy environment and improve detection efficiency, MSRA algorithm is proposed.

The MSRA perception algorithm model is illustrated in Figure 1. The perception model consists of M Second Users(SU) and a data Fusion Center(FC). The SU user is mainly responsible for (1) detecting the PU user's signal, (2) introducing the optimal SR in each path to improve the signal perception accuracy, (3) calculating the signal energy received by each SU for judgment, and (4) getting the judgment result. When an accurate judgment cannot be achieved, the FC will perform a weighted summation of the detection statistics from each path and compare it to a threshold value to elaborate the presence of the Primary User (PU).

Referring to the stochastic resonance-based single-node perception model, the statistical analysis of signal detection can be expressed as follows:

$$T_{SR}(r) = \sum_{n=0}^{N-1} |z_i(n)|^2, \quad (15)$$

when the sampling point N is large enough, the detection statistics follow the normal distribution. Therefore, the new equation is expressed as follows:

$$T_{SR} = \begin{cases} N\left(E_{0i}, D_{0i}\right), & H_0 \\ N\left(E_{1i}, D_{1i}\right), & H_1 \end{cases} \quad (16)$$

$$E_{0i} = N\left(\sigma_\omega^2 + \beta_i^2\right), \quad (17)$$

$$E_{1i} = N\left(\sigma_\omega^2 + \sigma_s^2\right) + N(\mu + \beta_i)^2, \quad (18)$$

$$D_1 = 2N\left(\sigma_\omega^2 + \sigma_s^2\right)^2 + 4N\left(\sigma_\omega^2 + \sigma_s^2\right)(\mu + \beta_i)^2, \quad (19)$$

Once the SU user calculates the detection probability of the signal, it is evaluated. If the detection rate exceeds or falls below the double-gate limit, it enables the identification of the PU signal. However, if it falls within the decision threshold range, it is subsequently transmitted to the data FC for further deliberation. The SU user will make a judgment to determine whether the PU exists. If the judgment fails, the FC will make a judgment. Therefore, the SU's decision model is given as follows:

$$Y = \begin{cases} H_0, & T_{SR}(r) \le \lambda_{low} \\ Not\ decide, & \lambda_{low} < T_{SR}(r) \le \lambda_{high} \\ H_1, & T_{SR}(r) > \lambda_{high} \end{cases} \quad (20)$$

Since the noise power in the real environment is dynamic, the actual noise $\hat{\sigma}_n^2$ conforms to the U $\left(\sigma_n^2/\rho, \rho\sigma_n^2\right)$ distribution, where ρ represents the uncertainty factor. The decision thresholds λ are obtained from Eq.(7), while the double thresholds λ_{low} and λ_{high} are respectively by λ and ρ

$$\lambda_{\text{low}} = \lambda/\rho, \quad (21)$$

$$\lambda_{high} = \lambda\rho, \quad (22)$$

When SU performs double threshold awareness, the detected information is transmitted to the FC using 2 bits, when the detection value of the SU node exceeds λ_{high}, it transmits a value of "11." Conversely, if the detection

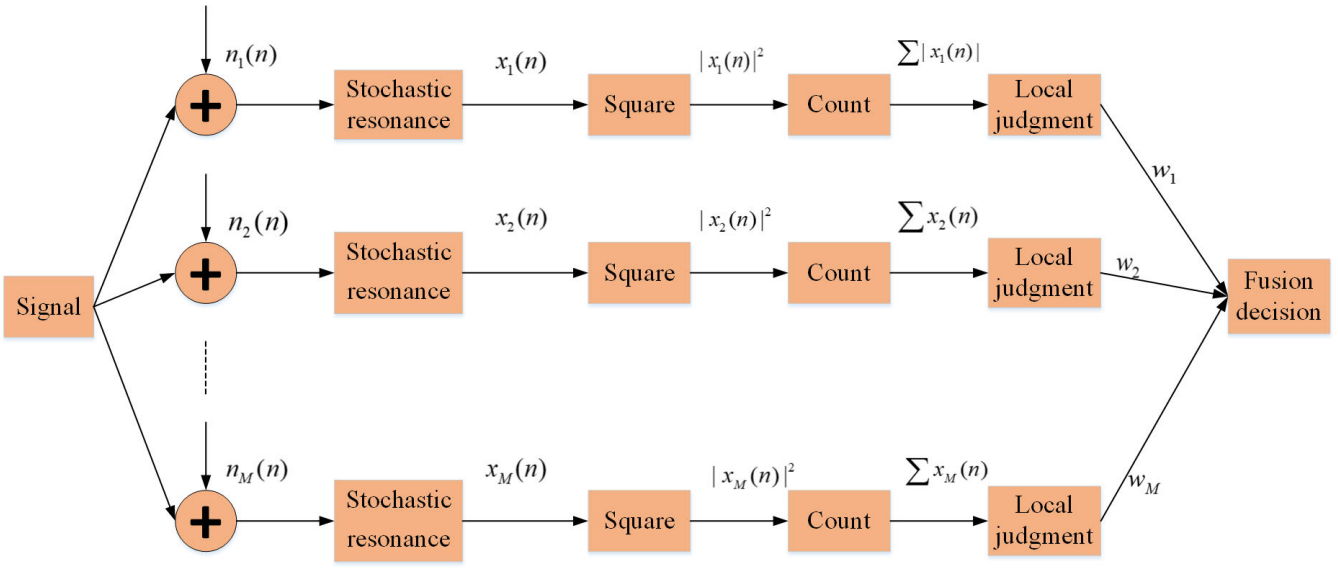

FIGURE 1. Multi-node collaborative perception model.

statistic falls below λ_{low}, it transmits a value of "10." In all other cases, a value of "00" is transmitted. The judgment criterion uses the OR criterion to decide, which can be expressed as follows:

$$D = \begin{cases} 1, & \sum_{i=1}^{N} E_i \geqslant 10 \\ 0, & \sum_{i=1}^{N} E_i < 10 \end{cases} \tag{23}$$

where E_i represents the bit transmitted by the i-th secondary user, while N denotes the total number of sensing nodes.

When the pass signal is not able to be detected by the random resonance double threshold energy detection algorithm, all the detection statistics are located between λ_{low} and λ_{high}, rendering it impossible for any SU to determine the presence of a PU. Consequently, each SU transmits its respective detection statistic T_i to the FC. In real-world settings, the presence of noise inevitably impacts the statistical analysis of the signal detection received by the FC. Therefore, the actual received detection statistics are as follows:

$$T_i' = T_i + n_i, \tag{24}$$

where n_i represents Gaussian white noise characterized by a zero mean and a variance of δ_j^2.

When defining about the existence of a PU, the judgment is typically made through a weighted fusion process. As different Sensing Units (SUs) are significantly affected by noise in real-world environments, it is critical for the algorithm to effectively optimize the weighting scheme. This involves assigning higher weights to sensing nodes with lower noise interference and smaller weights to those more affected by noise, thereby improving the accuracy of perception. The specific criteria for weight allocation are set as follows:

$$D_2 = \begin{cases} 1, & \sum_{i=1}^{L} \omega_i T_i' \geqslant \eta \\ 0, & 0 \leqslant \sum_{i=1}^{L} \omega_i T_i' < \eta \end{cases} \tag{25}$$

where w_i represents the weight of detection information for SU i. Moreover, the probabilities of false alarm and detection are denoted as follows:

$$P_i' = Q\left[\frac{\eta - \sum_{j=1}^{L} u\sigma_j^2\omega_j}{\sqrt{\sum_{j=1}^{L}\left(2u\sigma_j^4 + \delta_j^2\right)\omega_j^2}}\right], \tag{26}$$

$$P_d' = Q\left[\frac{Q^{-1}\left(P_{\mathrm{f}}\right)\sqrt{\sum_{j=1}^{L}\left(2u\sigma_j^4 + \delta_j^2\right)\omega_j^2} - \sum_{j=1}^{L} u\gamma_j\sigma_j^2\omega_j}{\sqrt{\sum_{j=1}^{L} 2\,u\left(1+2\gamma_j\right)\sigma_j^4\omega_j^2 + \delta_j^2\omega_j^2}}\right], \tag{27}$$

where γ_j represents the ambient SNR during data transmission from the i SU to the FC.

Based on the aforementioned false alarm probability and detection probability, it becomes clear that the detection probability is exclusively reliant on the weight when determining the SNR, false alarm probability, and energy. Therefore, the optimization problem primarily focuses on an optimizing process, defined as follows:

$$\max P_d' \tag{28}$$

$$\text{s. t.} \sum_{j=1}^{L} |\omega_j| = 1, \quad 0 \leqslant |\omega_j| \leqslant 1 \tag{29}$$

Algorithm 1 Collaborative Spectrum Sensing Pseudo-Code Based on Stochastic Resonance

```
input: N,number of sensing nodes,σ_w^2,σ_s^2, and δ
output: Channel state
procedure spectrum sensing(N,number of sensing nodes,σ_w^2,σ_s^2,δ)
    Perform single-node awareness
    for i ← 1toN do
        A single node perceives the channel(i)
    end for
    Fusion of multi-node sensing results
    if ( thenD == 0)
        Construct a multi-node collaborative perception model
        Using MSRA to solve the model
    end if
end procedure
```

The pseudo-code of the whole algorithm is as follows:

The weights selection is extremely important, and reasonable weight selection can better improve the perception effect of the algorithm. Concerning the weights selection, the QMROA is mainly applied. It will be introduced in detail in the next section.

IV. THE QUANTUM MANTA RAY OPTIMIZATION ALGORITHM

The Manta Ray Optimization Algorithm (MROA) is a novel optimization algorithm proposed in 2020, revealing stronger optimization capabilities compared to traditional heuristic algorithms [34]. In this work,the Quantum Manta-Ray Optimization Algorithm (QMROA) is proposed, leveraging quantum computing techniques to further enhance its optimization abilities. This algorithm consists of three components incorporating quantum operators and utilizing two states for representing an individual's position. Notably, improvements have been made to the chain-feeding and spiral-feeding operators to bolster global optimization capabilities and minimize the converging likelihood towards local optima.

A. QUANTUM REVOLVING GATE OPERATOR

Compared to other heuristic algorithms, quantum algorithms have significant differences. The most essential difference is that such algorithms mainly have quantum superposition properties and coherence properties. Moreover,in the quantum algorithm, the solution set of the heuristic algorithm does not consist of a fixed state, but a probability that there may be various states. In addition, the state matrix must be used for state transfer when the state is sent to transform.

The selection of the initial state in QMROA primarily relies on the use of the quantum revolving gate to address optimal solutions, thus emphasizing its significant impact on algorithm performance. The conventional equation for the quantum revolving gate is expressed as follows:

$$\begin{bmatrix} \alpha_{i,d} \\ \beta_{i,d} \end{bmatrix} = \begin{bmatrix} \cos\theta & -\sin\theta \\ \sin\theta & \cos\theta \end{bmatrix} \begin{bmatrix} \alpha_{i,d} \\ \beta_{i,d} \end{bmatrix} \tag{30}$$

where $\alpha_{i,d}$ is the value of the i manta ray in dimension d,$\beta_{i,d}$ is the value of d of the i manta ray in dimension β, $\alpha^2+\beta^2=1$ and θ is the quantum rotation angle.

The quantum rotation angle significantly impacts the algorithm, necessitating therefore an increase in the angle when there is minimal population differentiation. In the medium term, the gap is smaller, and the angle is reduced to ensure the population diversity. Therefore, the algorithm for the value of θ is described as follows:

$$\theta = e^{-step/iteration} + 0.01 \cdot ((Fit_i - (Fit_{\max} + Fit_{\min})/2) / (Fit_{\max} - Fit_{\min} + 0.000001)), \tag{31}$$

where the iteration represents the maximum number of iterations in the algorithm, Fit_{max} indicates the fitness of the individual with the highest fitness within the population, and Fit_{min} indicates the fitness of the individual having the lowest fitness among all individuals in the population.

In the aforementioned operator, as the discrepancy between the fitness of the current individual and that of the suboptimal individual with lower fitness within the population reduces, the Angle value also decreases. This adjustment aims to fine-tune the position of the current individual and prevent convergence towards local optima during subsequent population evolution stages.

B. ADAPTIVE WEIGHT OPERATOR

The MROA algorithm primarily depends of the chain feeding operator and spiral feeding operator for local updates, while flip feeding is employed to prevent convergence towards local optima. However, the MROA operator is susceptible to trapping in local optima during chain and spiral feeding update processes. This hinders the effectiveness of these updates in later population renewal stages and makes it challenging for the algorithm to yield an improved solution set. The operators in chain feeding and spiral feeding expressions are modified, mainly by adding adaptive update operators. The improvements are modelled as follows:

$$x_i^d(t+1,1) = \begin{cases} x_i^d(t,1) + r\left[x_{\text{best}}^d(t,1) - x_i^d(t,1)\right] + \\ 0.01 \cdot r \cdot \alpha\left[x_{\text{best}}^d(t-1,1) - x_i^d(t-1,1)\right] \ i=1 \\ x_i^d(t,1) + r\left[x_{i-1}^d(t,1) - x_i^d(t,1)\right] + \\ 0.01 \cdot r \cdot \alpha\left[x_{\text{best}}^d(t,1) - x_i^d(t,1)\right] \ i=2,\ldots,N \end{cases} \tag{32}$$

$$x_i^d(t+1) = \begin{cases} x_{best}^d + r(x_{best}^d(t) - x_i^d(t)) + \\ 0.01 \cdot r \cdot \alpha(x_{best}^d(t) - x_i^d(t)) \; i = 1 \\ x_{best}^d + r(x_{i-1}^d(t) - x_i^d(t)) + \\ 0.01 \cdot r \cdot \alpha(x_{best}^d(t) - x_i^d(t)) \; i = 2, \ldots, N \end{cases} \tag{33}$$

$$\alpha = \frac{1}{1 + e^{\sin(\pi/2 \cdot (x_{best}(i,1) - x_i(i,1))) + 5}}, \tag{34}$$

where $x_i^d(t, 1)$ denotes the α value of the i-th individual on dimension t, and $x_{best}(t, 1)$ represents the α value of the individual with the highest fitness on dimension t.

According to Eq.(34), a large fitness gap between the current population individual and the optimal individual indicates that the former has a significant α gap with respect to the latter, resulting in low fitness. In such cases, an increase in α value occurs. When updating using equations Eqs.(32) or (33), the current individual moves closer to achieving an optimal fitness. However, if there is a small surface gap between them despite the large fitness gap, the α value decreases. During population renewal, fine exploration around optimal individuals takes place without remaining too far from them.

C. SIMULATED ANNEALING UPDATE OPERATOR

The flipping foraging operator employed by MSRA primarily relies on the current position before moving to a new one. While this operator proves its efficiency during initial population renewal stages, it becomes imperative to engage in more refined exploration during the later stages to obtain a comprehensive solution set. Therefore, the flipping foraging operator may exert a greater adverse impact on overall population renewal. To enhance population diversity through judicious selection, the simulated annealing operator integrates flipping foraging with a certain probability. The specific formula is expressed as follows:

$$temp = x_i^d(t, 1) + S\left(r_2 \cdot x_{\text{best}}^d(t, 1) - r_3 \cdot x_i^d(t, 1)\right), \tag{35}$$

$$x_i^d(t+1, 1) = \begin{cases} temp, & rand < e^{-(Fit_i - Fit_{temp}) \cdot step/T} \\ x_i^d(t, 1), & other \end{cases} \tag{36}$$

where the fitness of the current individual, denoted as Fit_{temp}, is determined based on the number of current iterations.

V. EXPERIMENTAL RESULTS

In this section, the algorithm proposed in this paper is validated through simulation experiments. The simulation experiment assumes a single PU and one FC. To simulate the PU signal, a Binary Phase-Shift Keying (BPSK) signal with additive white Gaussian noise is applied. The average of the signal is set to 0.05, while the number of secondary users (SUs), denoted as M, is set to 60. Moreover, the sampling number N is designated as 2,000 and the probability of false alarm remains fixed at 0.1. The SNR for each SU and the data fusion center follows a random distribution within the $[-15, 0]$ dB range. Moreover, the Monte Carlo method is applied for conducting simulations exceeding 1500 iterations. Furthermore, an iterative process involving the QMRFA performed for 20 iterations. The obtained simulation results are shown below.

Algorithm 2 The Quantum Manta Ray Optimization Algorithm

```
input: Pouulation,T
output: Optimal individual
procedure optimization algorithm( Pouulation,T)
    Initialize the population randomly
    for t ← 1toN do
        if ( thenrand < 0.5)
            Perform a chain update.
        else
            if ( thenrand < t/T)
                Perform spiral foraging.
            else
                An individual is randomly generated for
                the spiral update.
            end if
        end if
        Simulated annealing operator update is per-
        formed.
        Perform quantum rotation gate. adjustment.
    end for
end procedure
```

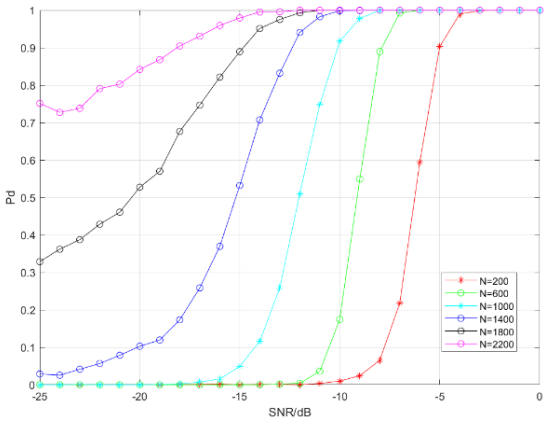

FIGURE 2. Correlation between the probability of detection and SNR across various sampling points in a multi-node scenario.

A. INFLUENCE OF SAMPLING POINTS ON ALGORITHM PERFORMANCE

The larger the number of sampling points is, the more accurate the perception will be. Therefore, the following experiments are conducted to verify the impact the of sampling points on the performance of the algorithm in both single node or multi-node perception models.

Figures 2 and 3 depict the variations in detection probability concerning signal-to-noise ratio (SNR) for

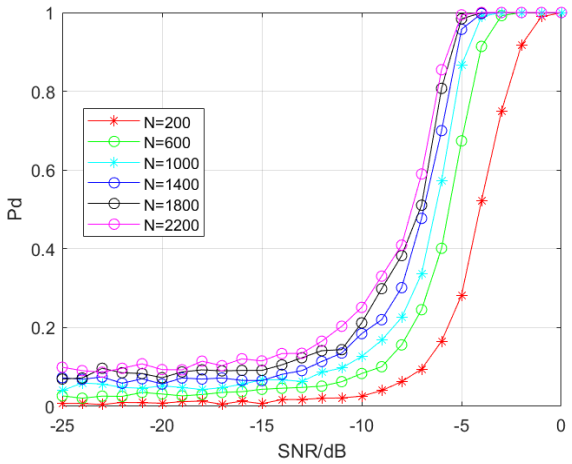

FIGURE 3. Correlation between the probability of detection and SNR across various sampling points in a single node scenario.

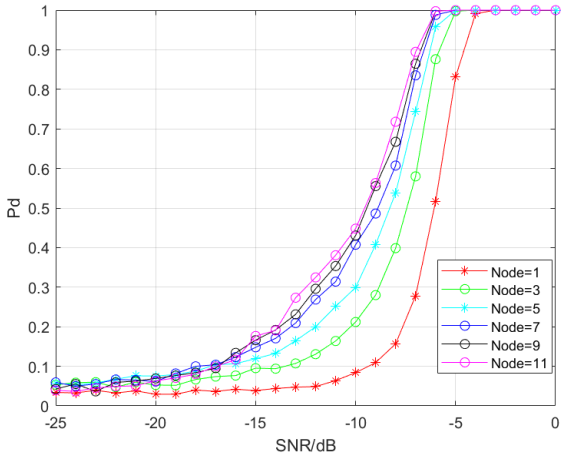

FIGURE 4. When N=1000, the detection probability varies with the SNR curve at different SU numbers.

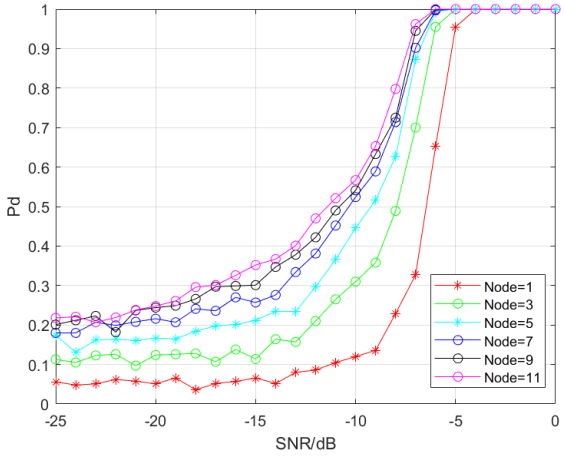

FIGURE 5. When N=1500, the detection probability varies with the SNR curve at different SU numbers.

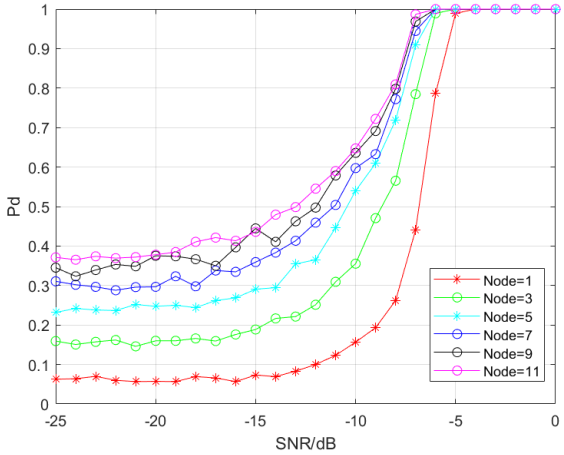

FIGURE 6. When N=2000, the detection probability varies with the SNR curve at different SU numbers.

different sampling points. Specifically, Figure 2 illustrates a multi-node collaborative sensing algorithm based on stochastic resonance, whereas Figure 3 denotes a single-node sensing algorithm also based on stochastic resonance. It is evident from both figures that, under constant conditions, an increase in the number of samples leads to an augmented detection probability. In the case of the single-node sensing algorithm, it can be noted that as the number of sampling points increases, the detection probability exhibits a diminishing improvement trend without yielding significant performance enhancement. As for in Figure 3, when $N = 1800$ and $N = 2200$, the disparity in performance between the two values becomes negligible, indicating that the sampling points no longer impose limitations on detection efficacy. Moreover, when N is 200, 600, 1000, and 1400, the detection performance is poor and the performance improvement effect is not obvious when N varies between -25 dB and -15 dB. However, when N is 1800 and 2200, the perception effect is significantly improved, mainly because the detection accuracy can be improved regarding the number of sampling points. However, it is not enough to improve the perception effect so significantly, mainly as the number of SU is 60 and the multi-node collaborative perception spectrum can significantly enhance the perception effect.

B. EVALUATE THE EFFECT OF THE NUMBER OF NODES ON ALGORITHM PERFORMANCE

The algorithm's performance is remarkably affected by the number of sensing nodes. While increasing this number may enhance algorithmic performance, it also imposes high demands on MSRA's solving capabilities. Therefore, it is questionable to know if reasonable weights can still be obtained as problem scale increases. Consequently, the following experiments describe the influence of the number of sensing nodes on the performance of the algorithm.

Figures 4, 5, and 6 depict the variation curve of detection probability with SNR for different numbers of SU users. Referring to these figures, under constant conditions, an increase in the number of SU users leads to a corresponding rise in the detection probability. This implies that augmenting the number of SUs can significantly enhance the detection probability; however, as the number of SUs

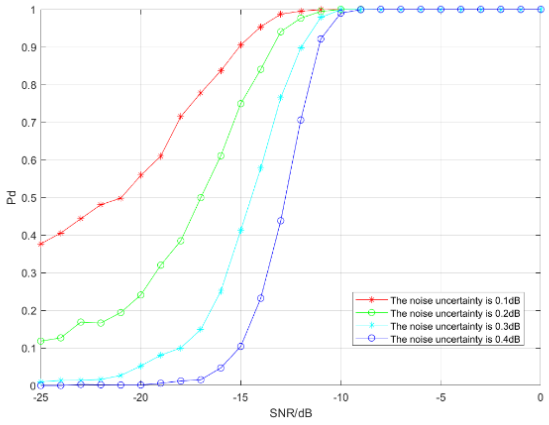

FIGURE 7. Change curve of detection probability with SNR under different noise uncertainty.

remains increasings, the improvement effect on spectrum sensing performance becomes progressively less noticeable. Concurrently,the increasing number of SU users is accompanied by an inevitable escalation in collaborative perception complexity. Henceforth, to ensure system operability within acceptable cooperation costs, it is obvious to judiciously select appropriate sensing nodes able to enhance detection performance even among challenging environments.

C. PERFORMANCE OF THE ALGORITHM UNDER DIFFERENT NOISE UNCERTAINTY

Noise uncertainty significantly influences the algorithm's performance, primarily because of the uncertain nature of the known noise variance in the model. In such cases, algorithms heavily relying on noise variance will experience substantial repercussions. Thus,this section primarily aims to experimentally validate the impact of noise variance on the algorithm performance.

Moreover,Figure 7 illustrates the variation curve of detection probability with SNR under different noise uncertainty levels. As depicted in the figure, an increase in noise uncertainty leads to a significant degradation in the performance of the detection. Specifically, when the level of noise uncertainty transitions from 0.1 to 0.2 dB, there is a noticeable decrease in detection performance. However, when the noise uncertainty moves from 0.3 to 0.4 dB, there is a notable deceleration in the attenuation of detection performance compared to the transition from 0.1 to 0.2 dB of noise uncertainty. Hence, it is clear that both noise uncertainty and SNR significantly impact the detection probability. In scenarios characterized by a high SNR ratio and low noise uncertainty, the algorithm demonstrates an elevated detection probability and achieves superior performance. Conversely, when faced with a low signal-to-noise ratio and significant noise uncertainty, the algorithm's detection probability significantly decreases, posing challenges in attaining improved performance levels.

To evaluate the performance of the proposed algorithm proposed in this paper under noise uncertainty, we employ two reference algorithms: the NTDED algorithm (a novel

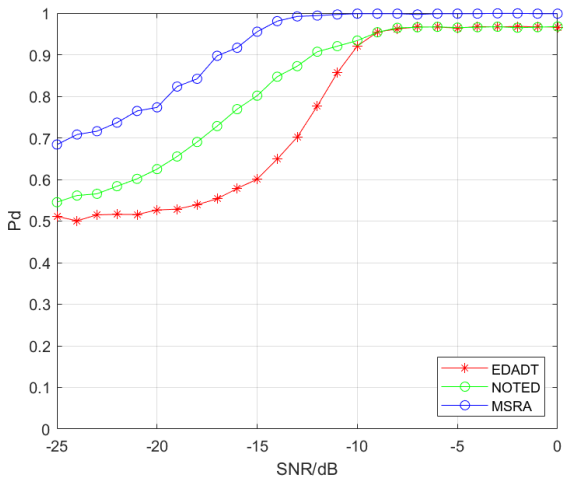

FIGURE 8. When the noise uncertainty is set at 0.1 dB, the detection probability exhibits variations by the SNR curve.

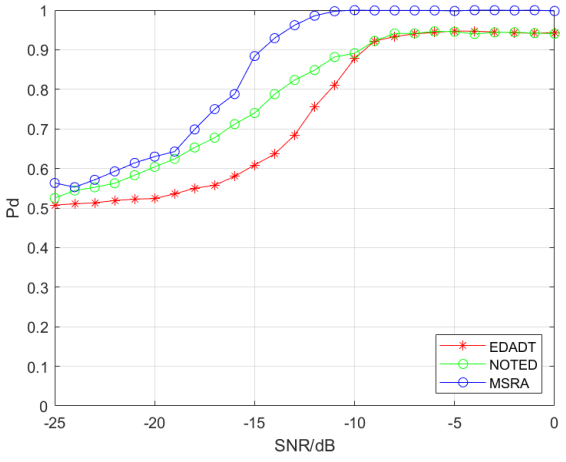

FIGURE 9. When the noise uncertainty is set at 0.2 dB, the detection probability exhibits variations by the SNR curve.

energy-based double threshold sensing algorithm) [35] and the EDADT algorithm (an adaptive double threshold algorithm) [36]. To assess different levels of noise uncertainties, the performance of our proposed algorithm with that of these two algorithms.

Furthermore,Figures 8, 9, 10, and 11 depict the detection performance under varying levels of noise uncertainty (0.1, 0.2, 0.3, and 0.4 dB). Notably, when the noise uncertainty is at its lowest level (i.e., at 0.1 dB), the proposed algorithm outperforms all other algorithms and achieves optimal detection results. However, as the noise uncertainty increases to higher levels (e.g., reaching 0.2 dB), the proposed algorithm still performs slightly better than the improved clustering detection algorithm;yet, it exhibits a significant decrease in the overall detection performance compared to that observed at lower levels of noise uncertainty (i.e., equal or below 0.1 dB). When the noise uncertainty is 0.3 and 0.4 dB, the performance of the algorithm proposed in this paper exhibits lower efficacy compared to EDADT and NTDED

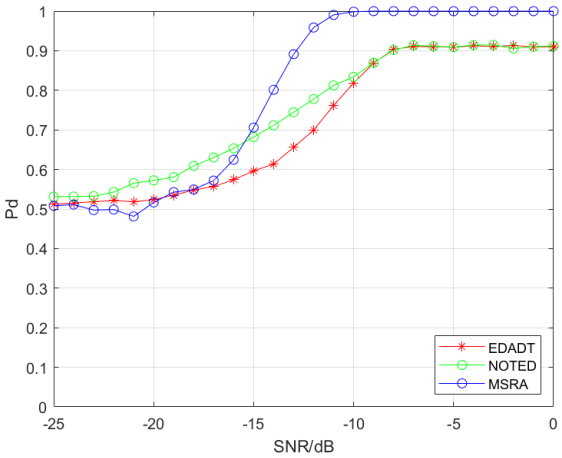

FIGURE 10. When the noise uncertainty is set at 0.3dB, the detection probability exhibits variations by the signal-to-noise ratio (SNR) curve.

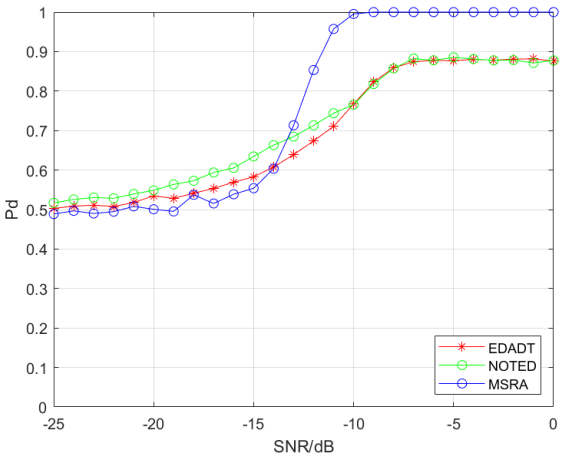

FIGURE 11. When the noise uncertainty is set at 0.4 dB, the detection probability exhibits variations by the SNR curve.

algorithms within the range of −25 and −15 dB. However, a partial improvement in performance is observed when compared to the enhanced clustering detection algorithm. The primary reason for the significant disparity between the proposed algorithm and EDADT/NTDED algorithms lies in constructing a multi-node cooperative perception model based on stochastic resonance, where information regarding the model has to be determined according to SNR considerations. In scenarios involving noise uncertainty, establishing a relatively reliable multi-node cooperative perception model becomes challenging.

The probability of a false alarm, denoted as P_f, plays a pivotal role in defining the performance of the detection probability. Specifically, the energy detection algorithm determines the threshold for either the energy detection algorithm or the double threshold energy detection algorithm based on P_f. Regarding our experimental setup, certain parameters are set as follows: when sensing the presence of PU, SU operate under an environmental SNR of −25 dB. Additionally, both SU and data FC experience a random

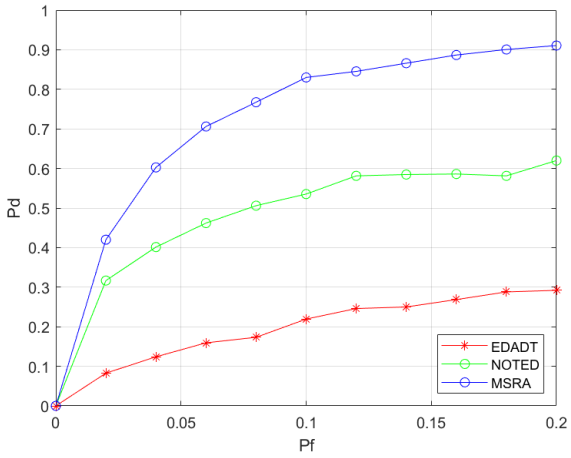

FIGURE 12. ROC curves of different energy detection algorithms.

SNR ranging from −20 dB to −15 dB. Therefore,Figure 12 illustrates how changes in false alarm probability the way the 0 to 0.02 affect the detection performance across four different algorithms.

D. EFFECT OF FALSE ALARM PROBABILITY ON ALGORITHM PERFORMANCE

The higher the false alarm probability is, the more evident the improvement in the algorithm performance will be. To evaluate the performance of different algorithms under varying false alarm probabilities,a series of experiments is conducted to assess the effectiveness of our proposed algorithm along with other novel approaches.

From the graph, it is evident that both the improved clustering detection algorithm and the NOTED algorithm exhibit similar performance. As the false alarm probability increases, the detection probability behaves in the same way. In comparison to these two other algorithms, the EDADT algorithm achieves superior detection performance, clearly surpassing the other three other algorithms. Notably, at $P_f = 0.2$, a more pronounced disparity in performance becomes apparent.

The proposed section introduces the QMRFO algorithm, exhibiting superior optimization capabilities compared to other crowd intelligence algorithms. To assess its performance, the algorithm was benchmarked against MRFO [34], Particle Swarm Optimization (PSO), and Reptile Search Algorithm (RSA) [37]. The number of sampling points is set to 1000, and the noise between the cognitive user and the FC follows a random distribution within the range of $[-25, 0]$dB. The are kept parameters remain unchanged. The experiment was repeated 30 times, and an average value was computed. Moreover, c_1 was set to 0.1 and c_2 was set to 0.2 in the PSO algorithm. ε was set to 0.1 and ω to 0.1 in the RSA algorithm. Finally,S is equal to 2 in the MRFO algorithm.

Moreover,Figure 13 shows that the PSO algorithm initially achieves good results with high detection probability in early iterations;however, it significantly lags behind MRFO and QMRFO algorithms in consequent optimization processes.

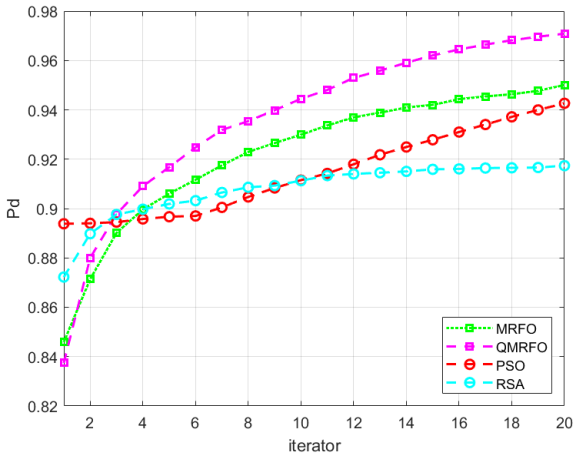

FIGURE 13. **Comparison of detection probabilities of different intelligent algorithms.**

In addition, the RSA algorithm exhibits strong global search capability, quickly achieving high detection probability in early iterations; however, it struggles to find better results after 10 iterations and is evidently inferior to the three other algorithms. Among these four algorithms,the QMRFO algorithm proposed in this paper demonstrates superior performance by attaining the highest detection probability and achieving optimal optimization effects for improved sensing results.

VI. CONCLUSION

The primary objective of this article consists of proposing a spectrum sensing algorithm. The algorithm achieves enhanced sensing performance in low SNR environments. Moreover, this work introduces stochastic resonance into a single node for perceiving the spectrum condition, thereby improving perception accuracy under low SNR conditions. However, it is important to solve the potential interference issues when relying on a single node for perception. To overcome such challenge, a multi-node collaborative perception algorithm is employed to mitigate interference problems. Furthermore, the QMROA algorithm is utilized to select optimal weights for the perception nodes to enhance the overall performance. Comparison through simulation experiments highlight that the proposed algorithm outperforms the other state-of-the-art perception algorithms, particularly in low SNR environments.

However, when confronted with high levels of noise uncertainty, the performance of this algorithm is subject to a significant decline, primarily during the multi-node cooperative sensing phase. Moreover, this phase relies on the accurate determination of sensing weights based on the SNR, becoming challenging under substantial noise uncertainty conditions. Consequently,a notable decrease in the algorithm performance is encountered. Therefore, future research should focus on enhancing algorithm performance under high noise uncertainty conditions. The proposed algorithm has inherent limitations when considering noise uncertainty. Additionally, when all SUs are unable to determine the existence of PUs, the FC must integrate sensing results from all SUs. In such cases, the collaborative sensing weight needs to be optimized using QMROA, requiring a certain amount of time to obtain appropriate weights. Consequently, it is not suitable for scenarios with high real-time requirements.

REFERENCES

[1] Y. Lin, Y. Tu, and Z. Dou, "An improved neural network pruning technology for automatic modulation classification in edge devices," *IEEE Trans. Veh. Technol.*, vol. 69, no. 5, pp. 5703–5706, May 2020.

[2] V. Srivastava, P. Singh, S. Mahajan, A. K. Pandit, A. M. Alshamrani, and M. Abouhawwash, "Performance enhancement in clustering cooperative spectrum sensing for cognitive radio network using metaheuristic algorithm," *Sci. Rep.*, vol. 13, no. 1, p. 16827, Oct. 2023.

[3] Y. Tu, Y. Lin, C. Hou, and S. Mao, "Complex-valued networks for automatic modulation classification," *IEEE Trans. Veh. Technol.*, vol. 69, no. 9, pp. 10085–10089, Sep. 2020.

[4] T. Umezawa and K. Akahane, "Application of high-speed photonic devices for fiber wireless and optical wireless communications," in *Proc. Opto-Electron. Commun. Conf. (OECC)*, Jul. 2023, pp. 1–2.

[5] H. R. D. Filgueiras, E. S. Lima, M. S. B. Cunha, C. H. De Souza Lopes, L. C. De Souza, R. M. Borges, L. Augusto Melo Pereira, T. Henrique Brandão, T. P. V. Andrade, L. C. Alexandre, G. Neto, A. Linhares, L. L. Mendes, M. A. Romero, and A. Cerqueira S., "Wireless and optical convergent access technologies toward 6G," *IEEE Access*, vol. 11, pp. 9232–9259, 2023.

[6] R. Salama, F. Al-Turjman, D. Bordoloi, and S. P. Yadav, "Wireless sensor networks and green networking for 6G communication- An overview," in *Proc. Int. Conf. Comput. Intell., Commun. Technol. Netw. (CICTN)*, Apr. 2023, pp. 830–834.

[7] M. Liu, H. Zhang, Z. Liu, and N. Zhao, "Attacking spectrum sensing with adversarial deep learning in cognitive radio-enabled Internet of Things," *IEEE Trans. Rel.*, vol. 72, no. 2, pp. 1–14, Sep. 2022.

[8] M. Wasilewska, H. Bogucka, and H. V. Poor, "Secure federated learning for cognitive radio sensing," *IEEE Commun. Mag.*, vol. 61, no. 3, pp. 68–73, Mar. 2023.

[9] Y. Lin, Y. Tu, Z. Dou, L. Chen, and S. Mao, "Contour stella image and deep learning for signal recognition in the physical layer," *IEEE Trans. Cognit. Commun. Netw.*, vol. 7, no. 1, pp. 34–46, Mar. 2021.

[10] Z. Yao, X. Fu, L. Guo, Y. Wang, Y. Lin, S. Shi, and G. Gui, "Few-shot specific emitter identification using asymmetric masked auto-encoder," *IEEE Commun. Lett.*, vol. 27, no. 10, pp. 2657–2661, Oct. 2023.

[11] C. Liu, X. Fu, Y. Wang, L. Guo, Y. Liu, Y. Lin, H. Zhao, and G. Gui, "Overcoming data limitations: A few-shot specific emitter identification method using self-supervised learning and adversarial augmentation," *IEEE Trans. Inf. Forensics Security*, vol. 19, pp. 500–513, 2024.

[12] Y. Lin, H. Zha, Y. Tu, S. Zhang, W. Yan, and C. Xu, "GLR-SEI: Green and low resource specific emitter identification based on complex networks and Fisher pruning," *IEEE Trans. Emerg. Topics Comput. Intell.*, pp. 1–12, 2024.

[13] N. Dewangan, A. Kumar, and R. N. Patel, "A framework for secure cooperative spectrum sensing based with blockchain and deep learning model in cognitive radio," in *Proc. Int. Conf. Artif. Intell. Knowl. Discovery Concurrent Eng.*, Jan. 2023, pp. 1–6.

[14] S. Lin, B. Zheng, F. Chen, and R. Zhang, "Intelligent reflecting surface-aided spectrum sensing for cognitive radio," *IEEE Wireless Commun. Lett.*, vol. 11, no. 5, pp. 928–932, May 2022.

[15] L. Li, W. Xie, and X. Zhou, "Cooperative spectrum sensing based on LSTM-CNN combination network in cognitive radio system," *IEEE Access*, vol. 11, pp. 87615–87625, 2023.

[16] C. M. Dharmapuri, N. Sharma, M. S. Mahur, and A. Jha, "Analysis of spectrum sensing techniques in cognitive radio," in *Computational Intelligence for Engineering and Management Applications: Select Proceedings of CIEMA 2022*, 2022, pp. 703–717.

[17] P. Gnanasivam, G. T. Bharathy, V. Rajendran, and T. Tamilselvi, "Efficient centralized cooperative spectrum sensing techniques for cognitive networks," *Comput. Syst. Sci. Eng.*, vol. 44, no. 1, pp. 55–65, 2023.

[18] K. Kockaya and I. Develi, "Spectrum sensing in cognitive radio networks: Threshold optimization and analysis," *EURASIP J. Wireless Commun. Netw.*, vol. 2020, no. 1, p. 255, Dec. 2020.

[19] N. Gul, M. S. Khan, S. M. Kim, J. Kim, A. Elahi, and Z. Khalil, "Boosted trees algorithm as reliable spectrum sensing scheme in the presence of malicious users," *Electronics*, vol. 9, no. 6, p. 1038, Jun. 2020.
[20] V. Devi, M. Monisha, M. Meena, E. N. Ganesh, R. Ramya, and T. Thirukkumaran, "Detection and sensing of cognitive radio spectrum using minimum eigen value and TW distribution method," in *Proc. Int. Conf. RECENT Innov. Sci. Technol.*, 2022, p. 20018.
[21] W. Wu, Z. Wang, L. Yuan, F. Zhou, F. Lang, B. Wang, and Q. Wu, "IRS-enhanced energy detection for spectrum sensing in cognitive radio networks," *IEEE Wireless Commun. Lett.*, vol. 10, no. 10, pp. 2254–2258, Oct. 2021.
[22] B. Bhavana, S. L. Sabat, S. Namburu, and T. Panigrahi, "Energy detector for spectrum sensing using robust statistics in non-Gaussian noise environment," in *Proc. 15th Int. Conf. Commun. Syst. Netw.*, Jan. 2023, pp. 414–418.
[23] M. Yang, Y. Li, X. Liu, and W. Tang, "Cyclostationary feature detection based spectrum sensing algorithm under complicated electromagnetic environment in cognitive radio networks," *China Commun.*, vol. 12, no. 9, pp. 35–44, 2015.
[24] D. Janu, K. Singh, and S. Kumar, "Machine learning for cooperative spectrum sensing and sharing: A survey," *Trans. Emerg. Telecommun. Technol.*, vol. 33, no. 1, p. e4352, Jan. 2022.
[25] S. Arya and Y. H. Chung, "Spectrum sensing for optical wireless scattering communications over Málaga fading—A cooperative approach with hard decision fusion," *IEEE Trans. Commun.*, vol. 69, no. 7, pp. 4615–4631, Jul. 2021.
[26] S. Nallagonda, A. Bhowmick, and B. Prasad, "Throughput performance of cooperative spectrum sensing network with improved energy detectors and SC diversity over fading channels," *Wireless Netw.*, vol. 27, no. 6, pp. 4039–4050, Aug. 2021.
[27] N. V. Barazande, R. Abdolee, B. M. Tazehkand, and H. Seyedarabi, "Energy efficient sensor selection method in cooperative spectrum sensing with low complexity," in *Proc. Wireless Telecommun. Symp. (WTS)*, Apr. 2018, pp. 1–6.
[28] X. Wu, Z. Tang, Y. Lu, D. Wu, H. Xiao, and Y. Tang, "Cooperative spectrum sensing method against spectrum sensing data falsification attack," in *Proc. 24st Asia–Pacific Netw. Operations Manage. Symp. (APNOMS)*, Sep. 2023, pp. 66–70.
[29] P. Yi, Z. Zhenyi, W. Xiang, and X. Zhaoping, "Cooperative spectrum sensing algorithm based on improved energy detection and sevcik fractal dimension," *Chin. J. Radio Sci.*, vol. 37, no. 6, pp. 1065–1072, 2022.
[30] H. Guo, W. Jiang, and W. Luo, "Linear soft combination for cooperative spectrum sensing in cognitive radio networks," *IEEE Commun. Lett.*, vol. 21, no. 7, pp. 1573–1576, Jul. 2017.
[31] Y. Lin, M. Wang, X. Zhou, G. Ding, and S. Mao, "Dynamic spectrum interaction of UAV flight formation communication with priority: A deep reinforcement learning approach," *IEEE Trans. Cognit. Commun. Netw.*, vol. 6, no. 3, pp. 892–903, Sep. 2020.
[32] Y. Lin, H. Zhao, X. Ma, Y. Tu, and M. Wang, "Adversarial attacks in modulation recognition with convolutional neural networks," *IEEE Trans. Rel.*, vol. 70, no. 1, pp. 389–401, Mar. 2021.
[33] W. Chen, J. Wang, H. Li, and S. Li, "Stochastic resonance noise enhanced spectrum sensing in cognitive radio networks," in *Proc. IEEE Global Telecommun. Conf.*, Dec. 2010, pp. 1–6.
[34] W. Zhao, Z. Zhang, and L. Wang, "Manta ray foraging optimization: An effective bio-inspired optimizer for engineering applications," in *Engineering Applications of Artificial Intelligence*, Jan. 2020.
[35] J. Zhu, H. S. Cao, J. Zhang, Z. S. Zhou, and Z. Qi, "Novel double threshold based energy detector for spectrum sensing," in *Proc. 6th Int. Conf. Signal Inf. Process., Netw. Comput.*, 2020, pp. 46–53.
[36] G. Mahendru, A. K. Shukla, and L. M. Patnaik, "An optimal and adaptive double threshold-based approach to minimize error probability for spectrum sensing at low SNR regime," *J. Ambient Intell. Humanized Comput.*, vol. 13, no. 8, pp. 3935–3944, Aug. 2022.
[37] L. Abualigah, M. A. Elaziz, P. Sumari, Z. W. Geem, and A. H. Gandomi, "Reptile search algorithm (RSA): A nature-inspired meta-heuristic optimizer," *Expert Syst. Appl.*, vol. 191, Apr. 2022, Art. no. 116158.

JUN CHEN received the M.Eng. degree in signal and information processing from the Huazhong University of Science and Technology, and his graduation thesis was rated as excellent. He is currently the General Manager of Chengdu Fuyuanchen Technology Company Ltd., where he leads research in high-speed array acquisition, broadband signal reception, and signal simulation.

YIPING HUANG received the B.Eng. degree in electronic information engineering from Chongqing University. He is currently the Deputy General Manager of Chengdu Fuyuanchen Technology Company Ltd., where he leads the technical team to complete the design and product delivery of signal processing boards and various types of receiver prototype prototypes.

TIANYI WANG received the M.Sc. degree from the College of Communication Engineering, University of Duisburg-Essen, in 2018. He is currently with China Research Institute of Radiowave Propagation. His research interests include knowledge graphs, digital signal processing, and artificial intelligence.

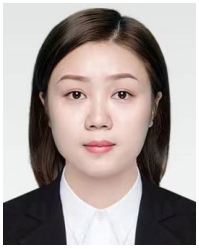

LING ZHANG received the M.Eng. degree in electronic science and technology (circuits and systems) from the School of Electronic Engineering, Xidian University. She is currently an Algorithm Engineer in the field of electronic countermeasures (ECM). Her research interests include signal-processing algorithms in the fields of electronic investigation and electronic interference.

YUQIAN LI received the M.Eng. degree from the College of Information and Communication Engineering, Harbin Engineering University, Heilongjiang, China, in 2021. She is currently with China Research Institute of Radiowave Propagation. Her research interests include signal time–frequency transform, image processing, and deep learning.